Environ Geol (2007) 52:399–407
DOI 10.1007/s00254-006-0473-0

ORIGINAL ARTICLE

Kaolinisation of granite in an urban environment

Nick Schiavon

Received: 2 June 2006 / Accepted: 16 August 2006 / Published online: 13 September 2006

Abstract Under natural acid and wet conditions, one of the main weathering processes affecting granitic rocks is the kaolinisation of Na, Ca and K-feldspar minerals by $H_2O + CO_2$ attack. We here report the occurrence of authigenic kaolinite on the surface of an eighteenth century granitic monument covered with sulphate-rich weathering patinas. We suggest that, in humid mesothermic climates, anthropogenically derived gaseous SO_2 from air pollution is responsible for accelerated kaolinisation of feldspars in an urban environment; SO_2 from air pollution thus plays a dual role in the weathering of silicate rocks being responsible for the well known sulphation of Ca-bearing materials leading to the formation of sulphate salts such as gypsum as well as the weathering of feldspar minerals to kaolinite. The kaolinisation reaction weakens the granite microfabric leading to enhanced decay of the building stone.

Keywords Granite · Urban environment · Sulphur dioxide · Feldspar · Kaolinite · Weathering

Introduction

Natural weathering processes can lead to the transformation of primary minerals in granitic rocks (s.l.) such as micas and feldspars into secondary crystalline and amorphous products. In wet, acid conditions, atmospheric attack on feldspar minerals is responsible for the formation of secondary clay minerals such as kaolinite ($Al_4(OH)_8[Si_4O_{10}]$) (Stoch and Sikora 1976; Yatsu 1988; Blum 1994; Wilson 2004); in a $CO_2 + H_2O$ rich atmosphere, the idealised stoichiometry of the kaolinisation reaction for orthoclase ($K[AlSi_3O_8]$) and albite ($Na[AlSi_3O_8]$) may be written as follows (Me = K, Na):

$$4Me[AlSi_3O_8] + 4H_2O + 2CO_2 \leftrightarrow Al_4(OH)_8[Si_4O_{10}] + 2Me_2CO_3 + 8SiO_2.$$

Blum (1994) subdivides the feldspar weathering process into two main stages, dissolution and precipitation; he states that "...feldspar weathering occurs via dissolution of all components, with the subsequent precipitation of secondary minerals from solution". Dissolution rates for feldspars are very slow and these rates are determining the overall weathering reaction rate. Feldspars of all compositions have dissolution rates that increases with decreasing pH at pH < 6. Other factors such as feldspar surface area (including internal surface area) and initial adsorption/exchange reactions also play an important role in the dissolution reaction. The weathering of feldspars under natural conditions is believed to be a process requiring 100,000 of years to complete (Blum 1994; Wilson 2004).

SO_2 attack on Ca-bearing porous building materials (such as, for example, limestones and/or lime mortars) with gypsum precipitation as an end product is well documented (Pye and Schiavon 1989; Lipfert 1989; Schiavon 1991, 1992; Fobe et al. 1995; Schiavon and Zhou 1996); although gypsum crystallisation on granitic building stone surfaces has also been ascribed to SO_2 air pollution, the detailed pathway of the chemical reactions leading to stone decay in low porosity

N. Schiavon (✉)
Department of Chemistry, University of Bologna,
via Selmi 2, 40126 Bologna, Italy
e-mail: nicola.schiavon@unibo.it

materials which contains less Ca (such as granitic stones) and are exposed to urban air pollution is less well understood (Schiavon et al. 1994, 1995).

As part of a wider investigation into the role played by SO_2-enriched urban atmospheres in the weathering of granite-forming silicate minerals (with special reference to feldspars), samples of surface patinas on granite walls from the eigthteenth century S. Jorge Church (Figs. 1, 2, 3, 4) have been collected in the town of La Coruña, Galicia, NW Spain. In this study, scanning electron microscopy (SEM) with energy-dispersive spectroscopy (EDS) and Fourier-transform infrared spectroscopy (FT-IR) have been combined to analyse in detail the weathering products and decay processes in the surface patinas of the S. Jorge church. One of the aims of the project was to assess whether gaseous SO_2 from air pollution can be directly responsible for the onset of chemical weathering reactions in feldspars and for corrosion of granitic building stones. Kaolinitised granite has been reported in urban monuments but it has so far been interpreted only as a decay feature inherited from natural weathering of the granite predating the use of the stone as building material (Begonha et al. 1994).

Materials and methods

Twenty patinas samples were collected from the granitic plinth at the base of the S-SW wall at approximately 1 m height (Figs. 2, 3, 4). The dark crusts sampled are composed of a framework of gypsum crystals ($CaSO_4{\cdot}2H_2O$) with fly ash and airborne soil particles (quartz and feldspar) as minor components. The stone is a fine grained leucogranite with polycrystalline quartz, xenomorphic K-feldspar, idiomorphic plagioclases and minor muscovite; plagioclase are more abundant than K-feldspars, biotitic mica is absent. The granitic stone shows weathering features such as dark patinas, white efflorescences, scaling and exfoiation features (Fig. 4). On the outskirts of the city of La Coruña, a high-sulphur lignite burning power plant is currently operational and air quality data for La Coruña province for 1986 show a mean SO_2 value of

Fig. 1 S. Jorge church, La Coruña (Galicia, Spain)

Fig. 2 S. Jorge church, La Coruña. Sampling area: granitic plinth at the base of the S-SW wall

Fig. 3 S. Jorge church, La Coruña. Sampling area: close-up of thin black sulphated layer on granitic surface. Note also the presence of whire powdery efflorescences on the same surface

Fig. 4 S. Jorge church, La Coruña; weathered granitic stone surface showing exfoliation and scaling

75 mg m^{-3}. The climate in the region is humid-mesothermic. Both rough specimen surfaces and polished thin sections of the granitic chips spanning the contact stone-patinas were microscopically examined. The thin sections were hand polished down to a thickness of 60–70 μm (thicker than the standard 30 μm used in routine petrographical analyses to account for differences in hardness between rock substrate and weathering patinas). After sputter coating with a thin carbon (thin sections) or gold (rough specimens) layer, samples were examined in a Jeol 820L SEM (with a Robinson back-scatter detector) interfaced with a Link 860 EDS system. Back-scattered electron imaging was used for thin-section work as it provides better image resolution when studying materials with a complex chemical/mineralogical composition such as the weathering patinas under investigation.

Powdered samples obtained by scraping with a stainless steel knife layers of black crusts and granitic substrate at increasing depths from the patinas-substrate interface were analysed by FT-IR spectroscopy (NICOLET 205 FT-IR Spectrometer). Infrared absorption spectra were obtained using KBr disks prepared by adding 1.5 mg of a pre-ground sample to 300 mg of potassium bromide (Aldrich FT-IR grade) and pressing it at a pressure of 9 tons for 4 min to form a 13 mm diameter disk 1.5 mm thick. FT-IR analysis provides information about the chemical nature of unknown compounds by recording the amount of stretching and bending vibrations of chemical bonds caused by the applied infrared radiation.

Results

Under SEM, sulphate patinas appear to be composed of a continuous, highly porous network of acicular, tabular and platy gypsum crystals. Within the gypsum framework, airborne iron-rich and aluminosilicate spherical particles and carbonaceous cenospheres derived from the combustion of fossil fuels can be seen together with mineral fragments detached from the rock substrate and soil dust (mainly well-rounded quartz grains). Although occasionally gypsum crystal enucleation seems to occur on the surface of carbonaceous anthropogenic particles typical of oil-fired power stations emissions, the bulk of sulphate precipitation does not show any correlation with the presence of these particles; furthermore their abundance in the sulphate patinas is very low. Physical weathering by gypsum crystal growth is evident, particularly on micas (muscovite) (Fig. 5); pre-existing fractures on quartz crystals are further enlarged by the enucleation and

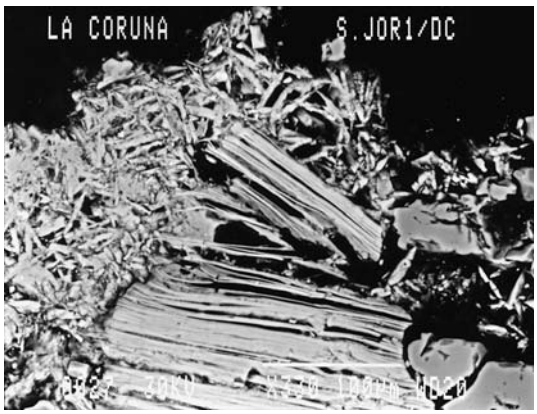

Fig. 5 S. Jorge church, La Coruña; granitic stone surface. Crystallisation of gypsum crystals along basal cleavage planes of mica mineral leads to physical decay of the stone. SEM micrograph, back-scattered image

growth of gypsum crystals. Gypsum crystallisation is observed down to a depth of a few millimeters from the original granite/atmosphere interface where it marks the inward boundary of the weathering front. Authigenic crystals of NaCl with a distinctive cubic habit may occasionally be found within the sulphate crust. Feldspars grains are generally absent from sulphate patinas and the weathered surface of the underlying granitic substrate. Where found, feldspar grains show the development on their surface of elongate etch trenches, striations and prismatic etch pits producing a pseudo-perthitic texture (Fig. 6). On the surface of the weathered granite and within the gypsum framework, micron-size poorly crystallised kaolinite occurring in aggregates and often displaying the distinctive booklet habit is common (Fig. 7); in EDS plots, these aggregates show an elemental spectrum with a low Si–Al

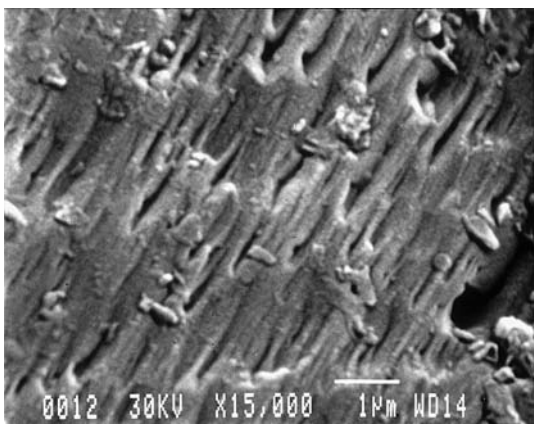

Fig. 6 S. Jorge church, La Coruña; interface granitic substrate/sulphate crust. Highly weathered feldspar surface. SEM micrograph, secondary image

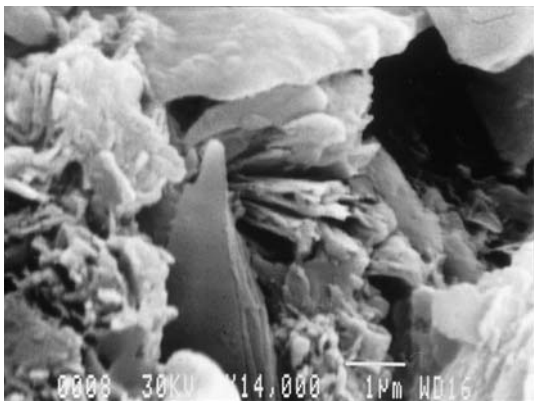

Fig. 7 S. Jorge church, La Coruña; granitic stone surface. Cluster of micron-size kaolinite crystals showing the typical booklet habit

peak ratio consistent with kaolinite chemical composition. Bulk X-ray diffraction analysis of sulphate patinas and of powdered samples obtained by scraping the outer surface of weathered granitic substrate confirms the presence of poorly crystallised kaolinite.

FT-IR results are summarised in Table 1, where a series of analytical wave number values (in cm^{-1}) of absorption bands from the FT-IR spectra of reference standards (gypsum, kaolinite, quartz, albite, orthoclase) and of powdered samples taken at increasing depths from the interface atmosphere/granitic surface (i.e. from black sulphate patinas down to unweathered granitic substrate) are listed. A typical example of FT-IR spectra of black sulphate crusts is shown in Fig. 8. By comparing FT-IR wavenumber values, relative intensities and peak shapes of unknown samples with the ones typical of pure compounds, we can establish whether the samples and the standards have (or have not) identical or very similar molecular structure and so verify the likely presence (or absence) of standard compounds in the unknown samples (Socrates 1994).

Table 1 shows the presence of kaolinite, gypsum and quartz (SiO_2) in samples 6–11 corresponding to black sulphate crusts (6), to the interface black crust/granitic substrate (7) and to samples at increasing distance (up to 2–3 mm) from the interface (8–11). The peak at $w = 3695\ cm^{-1}$ is characteristic of kaolinite and it is

Table 1 Absorption band values (wavenumbers in cm^{-1}) from FT-IR spectra of samples

1		3,548vs	1,685m	1143vs									670s	602
		3,407vs	1,621s	1,117vs										
2	3,697s				1,103vs		1,033vs	937m		788w		696m		
	3,620s						1,008vs	914s						
3														
								798		781	694			
4				1,139vs	1,094vs		1,031vs							
							1,012vs							
5				1,139vs		1053vs	-				770m			
							1,014vs							
6	3,695vs	3,547vs	1,685w	1,144vs			1,035vs	940w		788m		694m	670m	601sh
	3,621vs	3,407 vs	1,622 m	1,114vs			1010 vs	914 s						
7	3,697vs	3,548vs	1,686w	1,146vs			1,032vs			788m		694m	671m	602m
	3,620vs	3,406vs	1,621m	1,116vs			1,011vs	919s						
8	3,620vs	3,547vs	1,684w	1,147vs			1,034vs			787m		695w	670m	601m,s
	3,696vs	3,406vs	1,621m	1,116vs			1,011vs	919sh						
9	3,696s	3,540vs	1,684w1	1,144sh			1,034vs				780	693w	671m	601m,s
	3,620s	3,406vs	1,621m	1,114vs			1,009vs	914s						
10	3,696s	3,547vs	1,684w	1,146vs			1,034vs			786m		693w	671m	602s
	3,620s	3,406vs	1,621m	1,117vs			1,009vs	915s						
11	3,620m	3,545s	1,684w	1,144vs			1,034vs			786m		694w	671w	
	3,696m	3,406s	1,621m	1,116vs			1,010vs	916s						
12	3,620m	3,544s	1,684vw	1,144vs	1,096vs		1,036v1		797w	787m		695w	670w	
	3,696w	3,408s	1,621mw	-			1,016vs	919sh						
13	3,620m	-	-	1,143vs	1095vs		1035vs		797w	787m		695w		
	3,696w	3,410s	-	-			1,013vs	914s						
14				1,137vs	1,093vs	1,054vs,sh	1,041vs		798m		780m	695w		
							1,019vs							

1 standard gypsum, *2* standard kaolinite, *3* standard quartz, *4* standard albite, *5* standard orthoclase, *6* black sulphate crust, *7* interface black sulphate crust/granitic substrate, *8* granitic substrate (0.5–1 mm from interface), *9* granitic substrate (1–1.5 mm from interface), *10* granitic substrate (1.5–2 mm from interface), *11* granitic substrate (2–3 mm from interface), *12* granitic subtrate (3–4 mm from interface), *13* granitic substrate (5 mm from interface), *14* unweathered granitic substrate (>5 mm from interface). *w* weak, *s* strong, *vw* very weak, *vs* very strong, *m* medium, *sh* shoulder

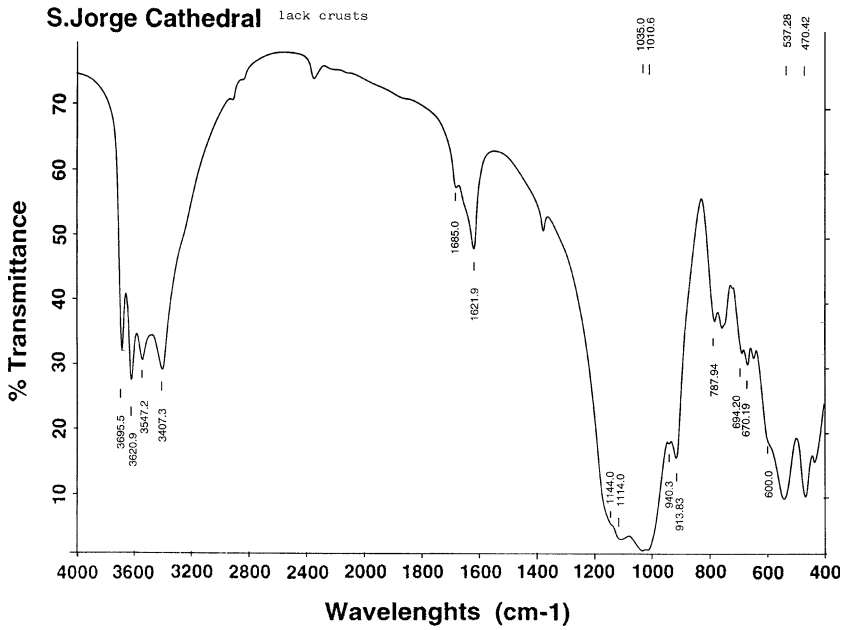

Fig. 8 S. Jorge church, La Coruña. Typical FT-IR spectrum of black sulphate crust. Numbers are wavenumbers in cm^{-1}

due to O–H stretching frequencies associated with the hydroxyl ions. A diagnostic pair of doublets for kaolinite (1035vs/1010vs cm^{-1} and 940m(sh)/914s cm^{-1}) is also present; the first one is due to Si–O and Al–Si–O bonding while the second one represents Al–O–OH bending of kaolinite (Lyon and Tuddenham 1960). Gypsum diagnostic peaks (which are interfering with main kaolinite peaks at w = 1112s cm^{-1} and at 1139vs/1117vs cm^{-1}) are at w = 3547vs, 3407vs cm^{-1} (OH stretching), 1685w, 1621s cm^{-1} (O–H–O bending of the crystallisation water) and at 1144vs (br, sh), 1114vs, 670 m, 600m(sh) cm^{-1} corresponding to the sulphate ions. Analytical wavenumber bands for silica (SiO_2) are in the range 690–800 cm^{-1} and represent the bending vibrational mode of the –Si–O–Si– bonds in the polymeric $(SiO_2)_n$ molecule. Within this range, there are differences between different silica compounds; Rao (1963) reports the following analytical wavenumbers: quartz = 694 cm^{-1}; quartz in industrial dust = 800 cm^{-1}; quartz in rocks = 781694 cm^{-1}. The reference values for quartz used in Table 1 (798, 780m, 695w cm^{-1}) derive from our own FT-IR analysis of a quartz standard. –Si–O–Si– bonds are also present in the kaolinite lattice between adjacent SiO_4 tetrahedra sharing oxygens and the absorption bands at 788w, 696m cm^{-1} in the kaolinite standard may be attributed to the vibrational bending mode of these bonds. On the other hand, the band at 787 cm^{-1} can also be ascribed to amorphous silica formed during kaolinisation of feldspars (Blum 1994), as it will be discussed below in the comments to Table 2.

In sample 12 (3–4 mm deep) kaolinite absorption bands are still present whereas gypsum bands decrease in intensity; at this depth, a well defined feldspar (albite) absorption band at 1096vs cm^{-1} appears for the first time together with a crystalline quartz band at 797 cm^{-1}. The first appearance of bands typical of granitic minerals shows that only partial kaolinisation occurred at this depth. In sample 13 (4–5 mm deep) gypsum bands disappear. At a depth of > 5 mm from the interface patinas/granite (sample 14, corresponding to the unweathered granite), the disappearance of kaolinite bands is associated with the appearance of well developed absorption bands typical of albite (1093 vs cm^{-1}), of orthoclase (1054vs, sh cm^{-1}) and of crystalline quartz (798 m, 780 m cm^{-1}) as the main constituents of the unaltered granitic stone. Although plagioclases, being part of a solid solution series between a calcic and a sodic end members (anorthite = An_{100}/Ab_0 and albite = An_0/Ab_{100} respectively) show a continuous compositional variation, we have experimentally observed, analysing plagioclase standards of various composition, that when An < 70%, only absorption bands typical of albite show up in FT-IR spectra. The mainly sodic composition of plagioclases in the granite used in the S. Jorge church thus explains the absence of anorthite bands in our FT-IR results corresponding to the unweathered granitic stone.

Table 2 reports the variation in intensity values (derived from transmittance values) along the weathering depth profile for selected absorption bands, chosen as representative of kaolinite (3696–7 cm^{-1}), of gypsum (670 cm^{-1}) and of amorphous silica + kaolinite (787 cm^{-1}); absorption wavenumber values for kaolinite standard are presented for comparison. The kaolinite band at 3696–7 cm^{-1} decreases in intensity from

Table 2 Trend of absorption band's intensity with increasing distance from interface atmosphere/granitic stone surface of characteristic bands of kaolinite (3696–7 cm^{-1}), gypsum (670 cm^{-1}) and of amorphous silica + kaolinite (787 (8) cm^{-1})

Spectrum	Sample	3696(7) cm^{-1}		670 cm^{-1}		787(8) cm^{-1}	
		%*T*	%*A*	%*T*	%*A*	%*T*	%*A*
2	Std kaolinite	28.3	71.7			58.3	41.7
6	black sulphate crust (bsc)	31.9	68.1	30.5	69.5	37.1	62.9
7	interface (if) bsc/substrate	33.8	66.2	20.9	79.1	17.4	82.6
8	substrate 0.5–1 mm from if	35.6	64.4	12.9	87.1	18.4	81.6
9	substrate 1–1.5 mm from if	42.5	57.5	25.7	74.3	25.0	75.0
10	substrate 1.5–2 mm from if	45.4	54.6	28.2	71.8	28.2	71.8
11	substrate 2–3 mm from if	59.3	40.7	38.5	61.5	36.5	63.5
12	substrate 3–4 mm from if	66.0	34.0	62.2	37.8	58.4	41.6
13	substrate 5 mm from if	68.0	32.0	-	-	63.0	37.0

T Transmittance *A* Absorbance Spectrum numbers as in Table 1. Bands intensity for kaolinite standard included for comparison. For discussion see text

surficial sulphate patinas to a depth of 5 mm from the interface gypsum patina/granite (samples 6–13). The gypsum band at 670 cm^{-1} shows a different trend: absorbance (i.e. intensity) increases up to a depth of 1 mm (samples 6–8); this is in agreement with SEM observations which show the depth of penetration of gypsum crystallisation (Fig. 2); the band's intensity then gradually decreases until it disappears at 5 mm from the interface (sample 13); it is important to note that, by contrast, kaolinite bands are still present at this depth showing how kaolinisation weathering fronts may penetrate deeper into the stone substrate than sulphate weathering fronts. The absorption band at 787 cm^{-1} which we interpret as representative of kaolinite + amorphous silica increases from the outer weathering patinas to the interface patina/granite (samples 6–7) and it then decreases to a depth of 5 mm (samples 8–13). The increase in band intensity in samples 6–7 could be ascribed to the presence, beside kaolinite, of amorphous silica released from weathering of feldspars (Blum 1994). There is indeed considerable evidence for the development of a Si-rich amorphous layer on the feldspar surface after dissolution in the acid region (pH < 3) (Berner and Holdren 1979). Other intermediate weathering products reported in laboratory simulation experiments (gibbsite, hydrargillite, halloysite) were not detected in the present investigation: whether this is due to their absence or their presence in amounts under the detection limits of the analytical techniques used is uncertain: their presence, however, is not necessary for the kaolinisation reaction as direct precipitation of kaolinite by feldspar hydrolysis with acid solutions (pH = 4) has been confirmed experimentally (Iglesia et al. 1976). Moreover, it has to be borne in mind that the present study is concerned with a ''real'' case study and is not a laboratory experimental study under controlled conditions and therefore not all the reaction phases need necessarily to be recorded in the weathering products.

Discussion

The kaolinite found on samples of granitic stone in the cathedral of S. Jorge in the town of La Coruña could have three main origins: (a) deposition of kaolinite-bearing airborne soil dust and/or surface wash on the building surface; (b) natural weathering in the original granite predating its use as a building stone; (c) authigenic formation as a result of weathering processes operating since the emplacement of the granite in the cathedral and its exposure to the urban atmosphere. The identification from FT-IR analysis of kaolinite absorption bands at depths of up to 4–5 mm from the interface surficial patinas-granitic stone rules out a soil dust or surface wash origin. On the other hand, the decreasing trend of kaolinite abundance in an inward direction from the surface of the granitic building stone until its disappearance at depths > 5 mm (Table 2) suggests that the kaolinite does not derive from weathering processes occurred during the granite's geological history. Moreover, feldspars from surface samples present etching pits and corrosion features (Fig. 6) consistent with the first step of feldspar weathering reaction, i.e. initial dissolution into solution (Berner and Holdren 1977; Baynes and Dearman 1978; Keller 1978; Blum 1994). The presence of kaolinite in S. Jorge church samples is then due to surface weathering of granitic building stone occurred *after* the emplacement of the stone in the cathedral. Kaolinization may affect both mica (biotite and muscovite) and feldspar minerals (Stoch and Sikora 1976; Yatsu 1988;

Blum 1994; Wilson 2004). The absence of biotite and the accessory nature of muscovite in the granite used in the building of S. Jorge, suggests that feldspars are the most likely ''reactants'' in the kaolinisation reaction.

SO_2 air pollution in a humid climate may be responsible for direct silicate weathering via heterogeneous attack of feldspars either by the aeriform mixture $SO_{2(gas)} + H_2O_{(vap)}$ adsorbed at the surface of the granite walls or by $SO2_{(aq)}$ in aqueous solution.

The reaction pathway may be subdivided in three steps and in the case of Ca-feldspar may proceed as follows:

(a) $2Ca(Al_2Si_2O_8) + 2SO_2 + 2H_2O = 2Ca\text{-}SO_3 + 2(Al_2Si_2O_8)^{2-} + 4H^+$ fast
(b) $2(Al_2Si_2O_8)^{2-} + 4H^+ = 2H_2(Al_2Si_2O_8)$ very fast
(c) $2H_2(Al_2Si_2O_8) + 2H_2O = Al_4(OH)_8(Si_4O_{10})$ very very slow

Steps (a) and (b) are in reality a unique fast reaction of ionic exchange between the cations Ca^{2+} and H^+ leading to the formation of calcium sulphite and of an acid aluminosilicate less stable than the reagent Ca-feldspar and has been reproduced in experimental weathering tests on Ca-rich feldspars (anorthite) whose results will be presented soon. Exchange and/or sorption reactions involving non framework cations such as K^+, Na^+ and Ca^{2+} are indeed one of the most common types of rapid surface reactions (the other being adsorption/desorption reactions involving dangling or bridging oxygens) occurring in experiments when unaltered feldspars are first placed in solutions (Blum 1994). The Ca^{2+} ions interleaving between the structural double layer of the silicate mineral, are esacoordinated with three oxygens atoms of one layer and with three oxygen atoms of the second layer. The calcium ions form six coordination bonds whereas the two H^+ do not and are then responsible for the metastable character of the acid aluminosilicate as compared with the feldspar. Step (c) is the slow rearrangement reaction of the acid aluminosilicate to a basic silicate of aluminium (kaolinite). Oxidation of the calcium sulphite in step (a) to sulphate (gypsum) may then ensue. Part of the gypsum present on sulphate crusts may then derive from sulphation of Ca-bearing minerals in the granite and not from reaction with lime mortars and/or limestone architectonic elements (Schiavon et al. 1995).

If we assume the attack to procede via $SO_{2(aq)}$, the reaction mechanism may be expected to follow a similar pathway to the one advocated for a $CO_{2(aq)}$ controlled weathering in natural systems, i.e. dissolution by aqueous, aggressive pore solutions and precipitation of kaolinite (Blum 1994); the stoichiometry for the latter reaction would indeed be similar with CO_2 substituting for SO_2. Simply to substitute CO_2 for SO_2 in the equation above, however, does not necessarily mean that the respective reactions need following identical pathways; the acid strengths of the dioxides are indeed different and experimental evidence is forthcoming in showing differences in the reactivity of CO_2 as compared with SO_2 in the simulated weathering of feldspar minerals. In a $CO_{2(aq)}$ controlled weathering mechanism the formation of kaolinite as one of the final products is believed to require 100.000 of years (Colman and Dethier 1984; Blum 1994; Wilson 2004); the reactivity differences mentioned above may influence the rate of the kaolinisation reaction and thus explain why in this study kaolinite is already present as a weathering product to a depth of 5 mm from the atmosphere/granitic stone interface after less than 100 years of exposure to a SO_2 aggressive atmosphere (corresponding to the time of significant SO_2 release in the Galicia region in northern Spain). Alternatively, to explain the presence of the final product of the reaction (i.e. kaolinite) in such a short time span, the decay reaction pathway may be thought as having been proceded through an heterogeneous attack by an aeriform mixture of $SO_{2\ (gas)} + H_2O_{\ (vapour)}$ adsorbed at the surface of the solid granite and not by $SO_{2(aq)}$. Kaolinite is found at depths of up to 4–5 mm from the granitic wall surface and the low porosity nature of granitic building stone (typical values for open porosity in granite are 0.2–0.3% in volume as opposed to values of up to 30% for limestones) and its low permeability is indeed unlikely to have allowed free circulation within the stone pore spaces of aggressive aqueous solutions in the same short time span considered in this study. Although microporosity has been shown to commonly exists in many unweathered feldspars (Walker 1990), the isolation of a large proportion of feldspar surface area in isolated micropores has been advocated to explain the one to three order of magnitude slower rate of feldspar natural weathering in field studies as compared with experimental studies (Veldel 1993); this further confirms how ''geological'' time is usually assumed to be needed for complete weathering to occur under a $CO_{2(aq)}$ aqueous solution driven mechanism. The corrosion mechanism by an aeriform mixture $SO_{2(gas)} + H_2O_{(vap)}$ here proposed may offset the inhibition effect on the rate of weathering caused by the above mentioned isolated nature of the microporosity and by preferential fluid flow considerations in feldspar minerals when dealing with dissolution in pore solution systems (Veldel 1993; Blum 1994). In summary, in a SO_2 polluted environment such is the case here considered, an aqueous solution does not need to

be a necessary condition for the initiation of chemical weathering on feldspars and of granitic stone decay.

The chemical and mineralogical transformation from aluminosilicate (feldspar, hardness = 6–6.5 on the Mohs scale) to basic silicate of aluminium (kaolinite, hardness = 2–2.5 on the Mohs scale) through the corrosion mechanism outlined above leads to important physical changes and significant weakening of the stone surface. The presence of minor kaolinite in well cemented quartz sandstones is known to be responsible for a decrease in the compression strenght and bulk density of the building stones (Sramek 1992). Kaolinisation of feldspars by SO_2 action acts together with gypsum crystallisation to promote loss of cohesion and spalling or flaking of the stone surface. The identification of kaolinite as a weathering product up to 4–5 mm from the stone/atmosphere interface beyond the level at which gypsum is found suggests that kaolinisation may penetrate even deeper into the stone substrate causing major stone decay. Recognition of this process has thus important applications in conservation science.

Conclusions

Authigenic kaolinite has been found on surface samples of granitic building stone in the town of La Coruña in northern Spain. Depth profiling of kaolinite abundance from the stone-atmosphere interface by FT-IR analysis suggests that kaolinite formed from weathering of the granite after exposure of the stone to the SO_2-enriched urban atmosphere in the last 100 years.

A model for the accelerated kaolinisation of feldpar minerals in granite is proposed which involves corrosion of the building stone via heterogeneous attack by an aeriform mixture of $SO_{2(gas)}$ + $H_2O_{(vap)}$ adsorbed at the surface of the granitic building stone. Taking into account the low porosity nature of granitic building stone, this reaction mechanism is preferred as opposed to the one promoted by $SO_{2(aq)}$ and is believed to better explain the presence of well formed kaolinite on the surface walls of a 200-year-old monument which have been exposed to significant SO_2 attack only for the past 100 years.

In the weathering of granitic building stone, SO_2 plays a dual role promoting both sulphate precipitation and kaolinisation of feldspars. Some of the Ca^{2+} ions needed for gypsum crystallisation may derive from plagioclase weathering; in laboratory simulated SO_2 attack on Ca-feldspar, Ca-sulphite and its oxidation product Ca-sulphate was obtained. Both processes have a profound effect in weakening the stone surface causing exfoliation, spalling and pulverisation.

Further research on SO_2 attack on granite is needed to establish whether kaolinisation is a general phenomenon in urban environments; future work will also include simulation experiments of granite weathering under laboratory controlled SO_2 concentrations.

Acknowledgments I would like to thank my late father, prof. Gaetano Schiavon, for endless and most fruitful discussions on the chemistry of SO_2 reaction and Prof. Benita Silva-Hermo of Departamento de Edafologia, University of Santiago de Compostela for useful discussions and help with the logistics of sampling.

References

Baynes J, Dearman WR (1978) The microfabric of a chemically weathered granite. Bull Int Assoc Eng Geol 18:91–100

Begonha A, Jeannette D, Hammecker C, Sequiera-Braga MA (1994) Physical characteristics of the Oporto Granite related to stone decay in monuments. In: Fassina V, Ott H, Zezza F (eds) The conservation of monuments in the Mediterranean Basin, pp. 541–546

Berner RA, Holdren GR (1977) Mechanism of feldspar weathering. Some observational evidence. Geology 5:369–372

Berner RA, Holdren GR (1979) Mechanism of feldspar weathering, II. Observations of feldspar from soils. Geochim Cosmochim Acta 43:1173–1186

Blum AE (1994) Feldspars in weathering. In: Parsons I (eds) Feldspars and their reactions. Kluwer, The Netherlands pp. 595–630

Colman SM, Dethier DP (1984) Rates of chemical weathering of rocks and minerals. Academic, London, p. 603

Fobe BO, Vleugels GJ, Roekens EJ,Van Grieken RE, Hermosin B, Ortega-Calvo JJ, del Junco AS, Saiz-Jimenez C (1995) Organic and inorganic components in limestone weathering crusts from cathedrals in southern and western Europe. Environ Sci Technol 29:1691–1701

Iglesia AL, Martin-Vivaldi JL, Aguayo FL (1976) Kaolinite crystallisation at room temperature by homogeneous precipitation, III. Hydrolysis of feldspars. Clays Clay Miner 24:36–42

Keller WD (1978) Kaolinisation of feldspar as displayed in scanning electron micrographs. Geology 6:184–188

Lipfert FW (1989) Atmospheric damage to calcareous stones. Comparison and reconciliation of recent experimental findings. Atmos Environ 23:415–429

Lyon RJP, Tuddenham WM (1960) Infrared determination of the kaolin group minerals. Nature 185:835–836

Pye K, Schiavon N (1989) Cause of sulphate attack on concrete, render and stone as indicated by sulphur isotope ratios. Nature 342:663–664

Rao CNR (1963) Chemical applications of infrared spectroscopy. Academic, London, p. 543

Schiavon N (1991) Gypsum crust formation and ''stratigraphy'' in weathered building limestones: a SEM study of stone decay in the UK. In C.Sabbioni NS Baer, A.J. Sors (eds.) Proceedings of the European Symposium ''Science & Technology for European Cultural Heritage'', Bologna, pp. 447–451

Schiavon N (1992) BSEM study of decay mechanisms in urban oolitic limestones. In: Robin GM. Webster (eds) Stone cleaning and the nature of soiling and decay mechanisms of stone. Donhead Publ, Edimburgh, pp. 141–151

Schiavon N, Chiavari G, Fabbri D, Schiavon G (1994) Microscopical and chemical analysis of black patinas on granite. In: Fassina V, Ott H, Zezza F (eds) Proceedings 3rd Int. Symp. The conservation of monuments in the mediterranean basin, Venice, pp. 93–99

Schiavon N, Chiavari G, Schiavon G, Fabbri D (1995) Nature and decay effects of urban soiling on granitic building stones. Sci Tot Envir 167:87–101

Schiavon N, Zhou LP (1996) Magnetic, chemical and microscopical characterization of urban soiling on historical monuments. Environ SciTechnol 30(12):3264–3629

Socrates G (1994) Infrared characteristic group frequencies. 2nd ed., Wiley, New York

Sramek I (1992) Kaolinitic quartz sandstones. The influence of mineralogy on physico-mechanical properties and durability. in Proceedings of the 7th International Congress on Deterioration and Conservation of Stone, LNEC Lisbon, 1:67–76

Stoch L, Sikora W (1976) Transformation of micas in the process of kaolinisation of granites and gneisses. Clays Clay Miner 24:156–162

Velbel MA (1993) Constancy of silicate mineral weathering rate ratios between natural and experimental weathering:implications for hydrologic control of differences in absolute rates. Chem Geol 105:89–99

Walker FDL (1990) Ion microprobe study of intergrain micropermeability in alkali feldspars. Contrib. Mineral Petrol 106:124–128

Wilson MJ (2004) Weathering of the primary rock-forming minerals: processes, products and rates. Clay Miner 39:233–266

Yatsu E (1988) The nature of weathering. Sozosha, Tokyo, p 624